Blue–green photoluminescence in MCM-41 mesoporous nanotubes

2003 J. Phys.: Condens. Matter 15 L297

(http://iopscience.iop.org/0953-8984/15/20/101)

INSTITUTE OF PHYSICS PUBLISHING JOURNAL OF PHYSICS: CONDENSED MATTER

J. Phys.: Condens. Matter **15** (2003) L297–L304 PII: S0953-8984(03)60779-4

LETTER TO THE EDITOR

Blue–green photoluminescence in MCM-41 mesoporous nanotubes

J L Shen[1,2,4], Y C Lee[1], Y L Lui[1], P W Cheng[3] and C F Cheng[2,3]

[1] Department of Physics, Chung Yuan Christian University, Chung-Li, Taiwan, Republic of China
[2] Centre for Nanotechnology at Chung Yuan Christian University, Chung-Li, Taiwan, Republic of China
[3] Department of Chemistry, Chung Yuan Christian University, Chung-Li, Taiwan, Republic of China

E-mail: jlshen@phys.cycu.edu.tw

Received 13 March 2003
Published 12 May 2003
Online at stacks.iop.org/JPhysCM/15/L297

Abstract

Different photoluminescence (PL) techniques have been used to study the blue–green emission from siliceous MCM-41 nanotubes. It was found that the intensity of the blue–green PL is enhanced by rapid thermal annealing (RTA). This enhancement is explained by the generation of twofold-coordinated Si centres and non-bridging oxygen hole centres, in line with the surface properties of MCM-41. On the basis of the analysis of the PL following RTA, polarized PL, and PL excitation, we suggest that the triplet-to-singlet transition of twofold-coordinated silicon centres is responsible for the blue–green PL in MCM-41 nanotubes.

1. Introduction

Mesoporous siliceous M41S materials such as MCM-41 and MCM-48 nanotubes have recently been synthesized and are attracting considerable attention [1]. These novel materials are synthesized via a liquid-crystal mechanism, where the structures can be formed by molecular aggregation of surfactants. The main characteristics of M41S materials are their high pore volume ($\sim$1 $cm^3\ g^{-1}$), large surface area ($\sim$1000 $m^2\ g^{-1}$), and very narrow pore-size distribution (2–10 nm). Much attention has been concentrated on these highly ordered structures due to their potential applications in heterogeneous catalysis, photocatalysis, adsorption, gas separation, and ion exchange [2–4]. While much of the academic and industrial research on M41S materials has focused on the synthesis procedures and chemical behaviours [5–7], there have been few investigations of the optical properties of these materials. The optical properties of mesoporous siliceous materials not only offer a convenient way to

[4] Author to whom any correspondence should be addressed.

clarify the nature of the structural defects, but also provide useful information for extending their range of applications in optical devices. The photoluminescence (PL) of mesoporous siliceous MCM-41 has been studied recently [8–13]. The red (1.8–2 eV) PL in MCM-41 has been commonly attributed to oxygen-related defects—non-bridging oxygen hole centres (NBOHCs) [8–10]. However, the origin of the blue–green (2.4–2.7 eV) PL in MCM-41 is still under debate and several models have been proposed. Gimon-Kinsel *et al* [8] first observed a green emission in as-synthesized and calcined MCM-41 powders and suggested that the radiative centres are related to the E′ centres or peroxyl radicals. Later, Zhang *et al* reported a broad PL, peaked at 477 and 512 nm, in calcined MCM-41. On the basis of the luminescence spectrum being similar to that of amorphous silica, that PL band was ascribed to twofold-coordinated silicon centres [11]. Chang *et al* [12] proposed another model to explain the blue–green (2.5–2.7 eV) PL in MCM-41; they demonstrated that the PL in MCM-41 can be interpreted on the basis of a transition of the Si–OH surface complex indicated by FTIR spectra and the persistent PL effect. Furthermore, Glinka *et al* assigned the green and blue PL from 6 nm sized mesoporous silica to hydrogen-related species [10] and self-trapped excitons [13], respectively. Obviously, the nature of the blue–green luminescence in MCM-41 is still an open question.

In this letter, we try to clarify the mechanism of generation of the blue–green PL in MCM-41 nanotubes by means of different PL techniques. On the basis of measurements of the PL following rapid thermal annealing (RTA), polarized PL, and photoluminescence excitation (PLE), we suggest that the blue–green PL in MCM-41 is due to a triplet-to-singlet transition of twofold-coordinated silicon on a surface, originating from the recombination of two surface E′ centres. An understanding of the optical properties of MCM-41 is expected to be important in the applications in photocatalysis and in the technological field of silica-based devices, such as light emitters [14], optical sensors, and optical memory bits [15].

2. Experimental details

The siliceous MCM-41 nanotubes studied here were synthesized using fumed silica (99.8%, metal free, Sigma), cetyltrimethylammonium (CTA) bromide (AR, 99%, Acros), and tetramethylammonium (TMA) hydroxide (25% aqueous solution, Aldrich). The syntheses of the siliceous MCM-41 were carried out according to the following procedure. (TMA)OH and (CTA)Br were added to deionized water while stirring at 30 °C until the solution became clear. The silica source was added to the solution while stirring for 2 h and then aged for 24 h. Gel mixtures with composition $1.00SiO_2$:0.19(TMA)OH:0.27(CTA)Br:$40H_2O$ were reacted for 48 h at 150 °C in Telflon-lined stainless steel autoclaves. The reaction product was filtered, washed with distilled water, and dried in air at 60 °C. Finally, the template was removed by calcination at 500 °C for 6 h. Some synthesized samples were further subjected to RTA in a pure N_2 environment. The RTA treatment was implemented using tungsten–halogen lamps at temperatures ranging from 200 to 800 °C for an annealing time of 30 s. Different PL techniques were used to investigate the MCM-41 samples. PL studies were performed at room temperature (RT) and using a He–Cd laser (325 nm) as the excitation source. PLE measurements were carried out with broadband light from a Xe lamp. The collected luminescence was dispersed by a grating spectrometer and detected with a cooled GaAs photomultiplier tube. For the polarized PL measurements, a linearly polarized He–Cd laser was normally incident on the sample surface and the luminescence was observed at right angles to the incident beam. The luminescence intensity was detected after passage through an analyser and the polarization of the luminescence was either parallel or perpendicular to the polarization of the incident beam.

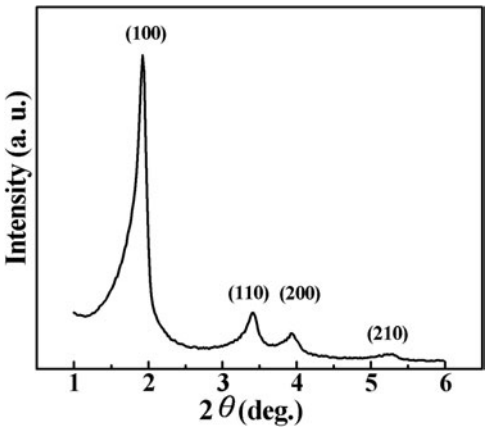

Figure 1. The x-ray diffraction pattern of the siliceous mesoporous MCM-41 nanotubes.

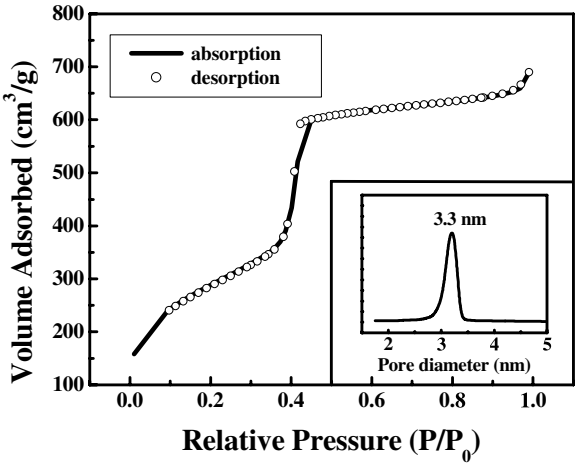

Figure 2. Isotherms of N_2 adsorption on siliceous mesoporous MCM-41 nanotubes. The inset shows the pore-size distribution curve.

3. Results and discussion

Figure 1 shows the x-ray diffraction pattern of our MCM-41 nanotubes. The diffraction pattern exhibits four clear peaks that can be indexed as (100), (110), (200), and (210) reflections. These features are consistent with a well-defined hexagonal honeycomb structure, which is the pattern characteristic of MCM-41. To analyse the pore-size distribution for the MCM-41 nanotubes, nitrogen adsorption–desorption measurements were carried out [16, 17]. A typical nitrogen sorption isotherm at 77 K is shown in figure 2. It corresponds to a reversible type IV isotherm, indicating the presence of mesopores. A sharp increase in the adsorbed and desorbed volumes at a relative pressure $P/P_0 \sim 0.42$ reflects the uniformity of the pore-size distribution. The average pore diameter calculated using the Barrett–Joyner–Halenda (BJH) method was very narrow at 3.3 nm [18, 19]. All these results indicate high quality for our MCM-41 samples.

Figure 3 shows the PL spectrum of as-synthesized MCM-41 nanotubes at RT. The spectrum displays a broad luminescence with the peak energy around 2.50 eV. Similar results have been reported in previous PL studies of MCM-41 [8, 11, 12]. We know of many structural models proposed for describing the mechanism of generation of the blue–green luminescence in MCM-41: E′ centres [8], peroxyl radicals [8], twofold-coordinated silicon centres [11], Si–OH

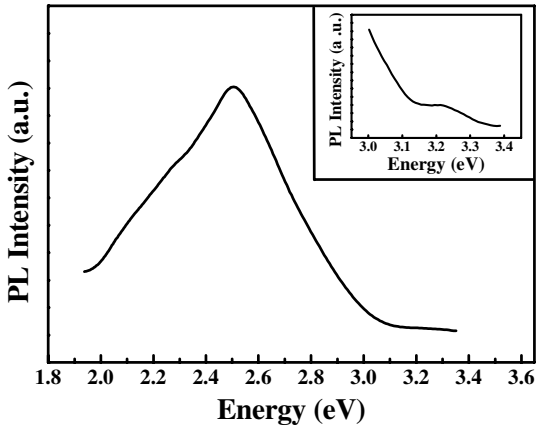

Figure 3. The PL spectrum of the as-synthesized MCM-41 nanotubes at RT. The inset shows the PL spectrum magnified, in the higher-energy region.

surface complexes [12], hydrogen-related species [10], and self-trapping of free excitons [13]. In order to clarify the origin of this blue–green luminescence, we performed PL studies in different situations. Figure 4 shows the PL spectra of MCM-48 before and after RTA treatment. It was found that the intensity of the 2.5 eV PL gradually increases as a function of the RTA temperature (T_{RTA}). In addition, another PL band peaked at 2.14 eV appears when $T_{\mathrm{RTA}} > 400\,^{\circ}\mathrm{C}$, and its intensity dominates for $T_{\mathrm{RTA}} = 800\,^{\circ}\mathrm{C}$ (figure 4(e)). The luminescence intensity after the RTA treatment with $T_{\mathrm{RTA}} = 800\,^{\circ}\mathrm{C}$ is about four times that of the untreated MCM-41. The enhanced luminescence of silica-based nanomaterials is of great interest because of its potential applications in light emitters in integrated optical devices [14] and the fluorescent read-out in optical memory bits [15]. From figure 4, we suggest that the blue–green PL in MCM-41 is strongly related to its surface properties. This is conceivable because the duration in the RTA treatment is very short (30 s), and the RTA effect should influence the sample surface only. In addition, MCM-41, due to its large surface area ($\sim$1000 $\mathrm{m^2\ g^{-1}}$), can provide lots of luminescent centres on its surface for generating PL. Now, in line with the surface properties of MCM-41, we try to analyse its PL following the RTA treatment. It is known that the MCM-41 surface is covered by silanol groups (Si–OH) of three kinds, i.e., single, hydrogen-bonded, and geminal silanol groups [20]. As the temperature is greater than RT, the hydrogen-bonded silanol groups in MCM-41 can be dehydroxylated by water removal and form siloxane bonds and single silanol groups [20, 21]:

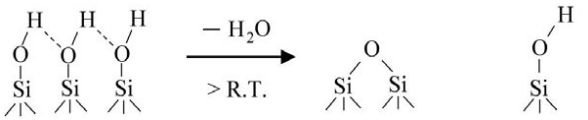

(1)

Dehydroxylation of the single silanol groups is considered to be impossible at this stage, since the distance between the single silanol groups is too large. Also, dehydroxylation of the geminal groups is very difficult since silicon does not form siloxane links readily [21]. Equation (1) indicates that still more water molecules on the MCM-41 surface can be removed by RTA treatment, and the concentration of single silanol groups thus increases upon RTA. Due to the removal of the water molecules, which perturb the emission from the luminescence centres on the surface, the PL intensity is therefore enhanced. The dehydroxylation of the hydrogen-bonded silanol groups dominates in the temperature range from RT to $T = 400\,^{\circ}\mathrm{C}$ and then decreases when $T > 400\,^{\circ}\mathrm{C}$ [21]. This explains the increased intensity of the 2.5 eV PL in MCM-41 for $T_{\mathrm{RTA}} < 400\,^{\circ}\mathrm{C}$.

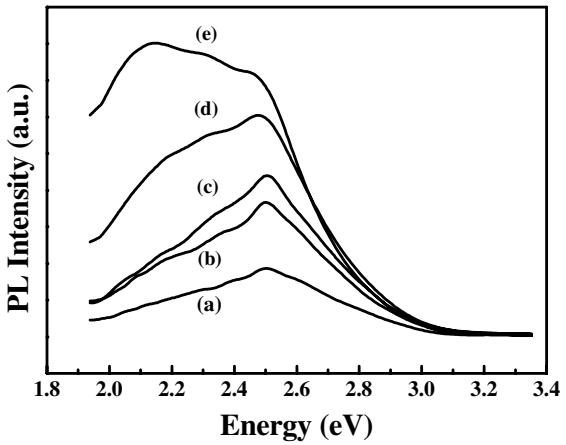

Figure 4. PL spectra of MCM-41 (a) as-synthesized; (b) after RTA at 200 °C; (c) after RTA at 400 °C; (d) after RTA at 600 °C; (e) after RTA at 800 °C.

For $T_{RTA} > 400\,^{\circ}C$, the dehydroxylation between single silanols with longer distance occurs and gives rise to the formation of strained siloxane bridges by the following process [21]:

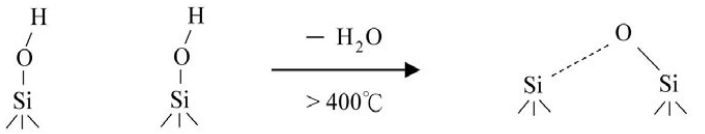

(2)

(strained siloxane bridge)

The strained siloxane bridge is unstable and has been demonstrated to create NBOHCs and surface E′ centres (i.e., $\equiv Si^{\cdot}$) through cleavage [22, 23]:

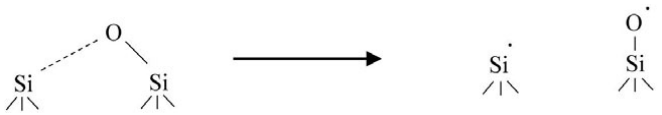

(3)

According to equations (2) and (3), both surface E′ centres and NBOHCs are expected to increase in concentration upon RTA treatment with $T_{RTA} > 400\,^{\circ}C$. Comparing with figure 4, we see that both NBOHCs and surface E′ centres are suitable candidates for being responsible for the blue–green PL. However, NBOHCs are believed to cause the red PL in silica [23–25], where the peak photon energy (∼1.9–2.2 eV) is significantly less than that (2.5 eV) of the blue–green luminescence here. On the other hand, according to the following process, similar to that in [26], the surface E′ centres can combine and produce twofold-coordinated silicon centres, which emit blue–green luminescence in a triplet-to-singlet transition:

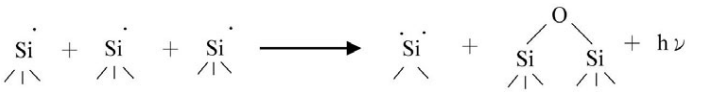

(4)

We therefore suggest that the blue–green PL in our MCM-41 is attributable to the triplet-to-singlet transition in twofold-coordinated silicon centres in equation (4). This assignment explains the enhanced blue–green luminescence after RTA with $T_{RTA} > 400\,^{\circ}C$, since the concentration of surface E′ centres in equation (3) is increased. Recently, the triplet-to-singlet luminescence energy of twofold-coordinated silicon centres has been found on the basis of first-principles calculations. The value obtained is 2.5 eV, which is in good agreement with

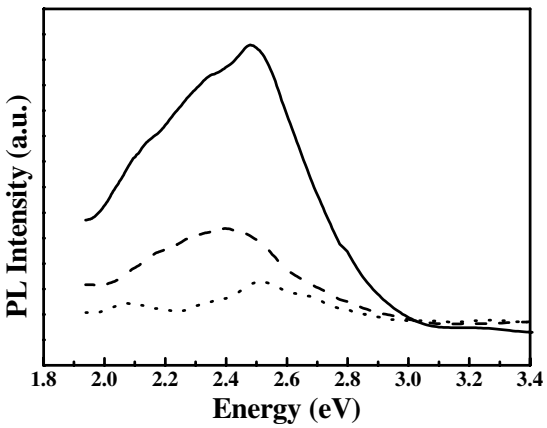

Figure 5. Polarized PL spectra of MCM-41 nanotubes. Dotted and dashed curves correspond to spectra with polarization of the PL parallel and perpendicular to the polarization of the incident beam. The solid curve represents the unpolarized PL spectrum. Due to the attenuation of light by the polarizer and analyser, the sum of the PL intensities of the dotted and dashed curves is smaller than the PL intensity of the solid curve.

our observation here [27]. The appearance of the 2.14 eV band in figure 4, curves (d), (e), can also be understood according to equation (3). As reported previously, NBOHC generation from different precursors may produce different emissions [28, 29]. Due to the cleavage from the strained siloxane bridges, the NBOHCs in equation (3) are in an environment of strain bonds. The PL energy of these NBOHCs (i.e., the NBOHCs associated with strained bonds) has recently been reported to be 2.19 eV [30], which is close to our observed value (2.14 eV) in figure 4. Therefore, the increased intensity of the 2.14 eV band may be due to the increased concentration of NBOHCs associated with strained bonds, arising from the precursor of the strained siloxane bridges.

To further investigate the PL properties of blue–green luminescence, polarized PL was measured. The degree of polarization, which relates to the preservation of the polarization between absorbing and emitting dipoles, can be obtained from a polarized PL measurement. The degree of polarization is defined by $P = (I_{\parallel} - I_{\perp})/(I_{\parallel} + I_{\perp})$, where $I_{\parallel}$ and $I_{\perp}$ are the intensities of the PL components polarized parallel ($I_{\parallel}$) and perpendicular ($I_{\perp}$) to the polarization of the incident beam. The theoretical maximum value of P in randomly oriented luminescence centres is 0.5, which indicates that the orientations of the absorbing and emitting dipoles are the same in the luminescence process [31]. P decreases if the orientation of the absorbing and emitting dipoles is not parallel. Different luminescent defect centres (defined as defect centres which can produce radiative luminescence after optical excitation) hence yield different P-values due to their specific defect structures. Thus, the degree of polarization P provides a basis for identifying the luminescent defect centres. Polarized PL spectra obtained from MCM-41 nanotubes are shown in figure 5. The dotted and dashed curves in figure 5 correspond to the spectra with the polarization of the PL parallel and perpendicular to the polarization of the incident beam. The degree of polarization P at 2.5 eV calculated from figure 5 was found to be 25%, which agrees well with the P-value (22%) obtained for the reported triplet-to-singlet transition in twofold-coordinated silicon [32]. Obviously, the polarization property of blue–green PL in MCM-41 is consistent with our assignment.

Another useful technique for investigating the physical nature of the luminescence signal is that of PLE, which measures the excited levels or bands of the system by detecting the photon energy at the emission band. In the PLE mechanism, the luminescence intensity is proportional to the number of photogenerated carriers, which is in turn proportional to the absorption. Therefore, PLE studies not only give us the absorption properties of MCM-41, but also provide useful information for applying mesoporous materials as optical sensors, absorbers, and photocatalysts. However, to our knowledge, no PLE studies on MCM-41 or

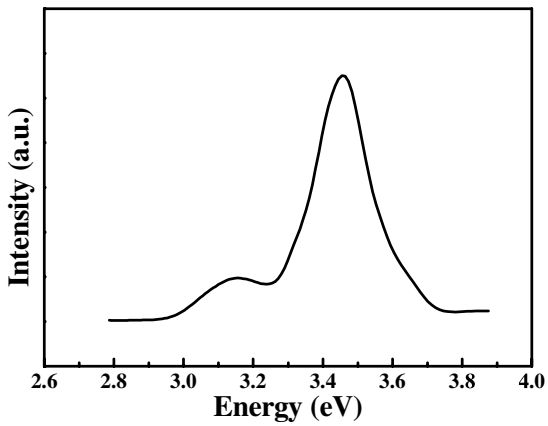

Figure 6. The PLE spectrum of the 2.5 eV emission band for MCM-41 nanotubes.

other mesoporous M41S materials have been reported. The PLE spectrum of the 2.5 eV emission band is presented in figure 6, showing a main peak at 3.47 eV and a small peak at 3.13 eV. The energy of the main peak approaches the calculated values for the direct singlet-to-triplet excitation transition in twofold-coordinated Si, which are 3.3 [33] and 3.6 eV [34] based on the oxygen vacancy and cluster models, respectively. Again, the optical excitation property of the blue–green PL in MCM-41 nanotubes is consistent with our assignment. The smaller 3.13 eV peak is also observable in the PL spectrum (see the inset of figure 3). This peak has been observed for many forms of silica and related to a twofold-coordinated Ge impurity [35], the O_2^- intrinsic defect [36], and the –O–O– type of defect [37]. To achieve further understanding of the 3.13 eV peak, we have performed PL measurements in an O_2 atmosphere. It was found that the PL intensity of the 3.13 eV peak is different for the measurements in the O_2 ambient (not shown). Therefore, the 3.13 eV excitation peak may relate to an oxygen-type defect, although the exact origin is not clear at present.

Recently, it has been reported that the blue PL band of mesoporous silica is attributable to the triplet-to-singlet transition of self-trapped excitons [13]. Self-trapped excitons are electron–hole pairs localized at a self-induced lattice distortion, resulting from strong electron–phonon interactions. The luminescence energy emitted from self-trapped excitons for crystalline and amorphous silica is around 2.6–2.8 eV [25, 38] and 2.4 eV [39], respectively. These energies are close to our observed PL value (2.5 eV) for MCM-41. However, we deduce that the 2.5 eV PL band of our MCM-41 should not come from self-trapped excitons, because the measured excitation transition energy (3.47 eV) in figure 6 is far below the energy ($\sim$9 eV) needed to generate self-trapped excitons in silica. This implies that blue luminescence has not originated from self-trapped excitons for our MCM-41.

4. Conclusions

In summary, the blue–green PL of mesoporous MCM-41 nanotubes was investigated using different PL techniques. The intensity of blue–green PL was found to be enhanced by RTA treatment, suggesting potential applications in light-emitting and optical memory devices. The enhancement is explained by the generation of twofold-coordinated Si centres and NBOHCs in line with the surface properties of MCM-41. Through the analysis of polarized PL, it was found the blue–green PL centres are anisotropic with a degree of polarization of 0.25. In addition, we performed PLE studies of MCM-41 for the first time, finding a main excitation band of blue–green emission at 3.47 eV. On the basis of the above PL studies, we strongly

suggest that the blue–green PL in MCM-41 nanotubes is due to a triplet-to-singlet transition of twofold-coordinated silicon centres. The studies presented here are expected to be useful for clarifying the nature of light emission in MCM-41 and to be of practical use due to its possible applications in optical devices and as a photocatalyst.

This project was supported in part by the National Science Council under the grant numbers 91-2112-M-033-012 and 91-2745-M-033-001.

References

[1] Kresge C T, Leonowicz M E, Roth W J, Vartuli J C and Beck J S 1992 *Nature* **359** 710
[2] Kageyama K, Tamazawa J and Aida T 1999 *Science* **285** 2113
[3] Stein A, Melde B J and Schroden R C 2000 *Adv. Mater.* **12** 1403
[4] Corma A 1997 *Chem. Rev.* **97** 2373
[5] Cheng C F, Zhou W, Park D H, Klinowski J, Hargreaves M and Gladden L F 1997 *J. Chem. Soc. Faraday Trans.* **93** 359
[6] Park S E, Kim D S, Chang J S and Kim W Y 1998 *Catal. Today* **44** 301
[7] Kumar D, Schumacher K, du Fresne von Hohensche C, Grun M and Unger K K 2001 *Colloids Surf.* A **187/188** 109
[8] Gimon-Kinsel M E, Groothuis K and Balkus K J Jr 1998 *Micropor. Mesopor. Mater.* **20** 67
[9] Shen J L, Chen P N, Lee Y C, Cheng P W and Cheng C F 2002 *Solid State Commun.* **122** 65
[10] Glinka Yu D, Zyubin A S, Mebel A M, Lin S H, Hwang L P and Chen Y T 2002 *Chem. Phys. Lett.* **358** 180
[11] Zhang Y, Phillipp F, Meng G W, Zhang L D and Ye C H 2000 *J. Appl. Phys.* **88** 2196
[12] Chang H J, Chen Y F, Lin H P and Mou C Y 2001 *Appl. Phys. Lett.* **78** 3791
[13] Glinka Yu D, Lin S H, Hwang L P and Chen Y T 2000 *J. Phys. Chem.* B **104** 8652
[14] Yu D P, Hang Q L, Ding Y, Zhang H Z, Bai Z G, Wang J J, Zou Y H, Qian W, Xiong G C and Feng S Q 1998 *Appl. Phys. Lett.* **73** 3076
[15] Sun H B, Juodkazs S, Watanabe M, Matsuo S, Misawa H and Nishii J 2000 *J. Phys. Chem.* B **104** 3450
[16] Ciesla U and Schuth F 1999 *Micropor. Mesopor. Mater.* **27** 131
[17] Schumacher K, Grun M and Unger K K 1999 *Micropor. Mesopor. Mater.* **27** 201
[18] Barrett E P, Joyner L G and Halenda P P 1951 *J. Am. Chem. Soc.* **73** 373
[19] Kruk M, Jaroniec M and Sayari A 1997 *Langmuir* **13** 6267
[20] Zhao X S, Lu G Q, Whittaker A K, Millar G J and Zhu H Z 1997 *J. Phys. Chem.* B **101** 6525
[21] Inaki Y, Yoshida H, Yoshida T and Hattori T 2002 *J. Phys. Chem.* B **106** 9098
[22] Devine R A B and Arndt J 1990 *Phys. Rev.* B **42** 2617
[23] Kajihara K, Skuja L, Hirano M and Hosono H 2001 *Appl. Phys. Lett.* **79** 1757
[24] Skuja L 1994 *J. Non-Cryst. Solids* **179** 51
[25] Kalceff M A S and Phillips M R 1995 *Phys. Rev.* B **52** 3122
[26] Skuja L 1998 *J. Non-Cryst. Solids* **239** 16
[27] Zhang B L and Raghavachari K 1997 *Phys. Rev.* B **55** R15993
[28] Nagasawa K, Ohki Y and Hama Y 1987 *Japan. J. Appl. Phys.* **26** L1009
[29] Glinka Yu D, Lin S H and Chen Y T 2000 *Phys. Rev.* B **62** 4733
[30] Griscom D L and Mizuguchi M 1998 *J. Non-Cryst. Solids* **239** 66
[31] Skuja L, Tanimura K and Itoh N 1996 *J. Appl. Phys.* **80** 3518
[32] Skuja L, Streletsky A N and Pakovich A B 1984 *Solid State Commun.* **50** 1069
[33] Skuja L 1992 *J. Non-Cryst. Solids* **149** 77
[34] Pacchioni G and Ierano G 1997 *J. Non-Cryst. Solids* **216** 1
[35] Skuja L N, Truhin A N and Plaudis A E 1984 *Phys. Status Solidi* a **84** K153
[36] Guzzi M, Martini M, Mattaini M, Pio F and Spinolo G 1987 *Phys. Rev.* B **35** 9407
[37] Nishikawa H, Shiroyama T, Nakamura R, Ohki Y, Nagasawa K and Hama Y 1992 *Phys. Rev.* B **45** 586
[38] Itoh C, Tanimura K and Itoh N 1988 *J. Phys. C: Solid State Phys.* **21** 4693
[39] Tanimura K, Itoh C and Itoh N 1988 *J. Phys. C: Solid State Phys.* **21** 1869